COHERENT STRUCTURES IN A POPULATION MODEL FOR MUSSEL-ALGAE INTERACTION.

ANNA GHAZARYAN AND VAHAGN MANUKIAN

Abstract. We consider a known model that describes formation of mussel beds on soft sediments. The model consists of nonlinearly coupled pdes that capture evolution of mussel biomass on the sediment and algae in the water layer overlying the mussel bed. The system accounts for the diffusive spread of mussel, while the diffusion of algae is neglected and at the same time the tidal flow of the water is considered to be the main source of transport for algae, but does not affect mussels. Therefore both the diffusion and the advection matrices in the system are singular. A numerical investigation of this system in some parameter regimes is known. We present a systematic analytic treatment of this model. Among other techniques we use Geometric Singular Perturbation Theory to capture nonlinear mechanisms of pattern and wave formation in this system.

1. Introduction

The ability of mussels to self-organize has been known to the ecologists (see [13] and references within). In recent years, there is a significant interest towards using mathematics to understand the mechanisms of the phenomenon of aggregation and pattern formation in mussel beds is noticeable. Predator-prey models have been suggested to explain pattern formation in mussel beds. Some of them are restricted to mussel and algae interactions [13, 14], some, in addition, include a description of sediment accumulation [10]. In [9] Cahn-Hilliard equation has been demonstrated to successfully capture patterns observable in experiments which points out the role of the phase separation in mussel pattern formation. In this paper we concentrate on the two-component partly parabolic system of partial differential equations described below.

Van der Kopel and collaborators in [13] introduced the following system as a model for predator-prey interaction between algae and mussels with a linear functional response,

$$\begin{aligned} A_\tau &= (A_{up} - A)f - \frac{c}{h}AM - \nu A_x, \\ M_\tau &= ecAM - d_M \frac{k_m}{k_m + M} M + D(M_{xx} + M_{yy}). \end{aligned} \tag{1.1}$$

Here $A = A(x, y, \tau)$ is the concentration of algae in the water layer and $M = M(x, y, \tau)$ is the mussel biomass per square meter of sediment surface, (x, y) is the two-dimensional space representing sediment surface, τ is the time. All of the constants in this model are

Date: December 19, 2013.

non-negative. A_{up} is the concentration of algae in the upper water level, f is the rate of exchange between the lower and upper levels, c is the consumption constant, h is the height of the lower water level, e is the conversion constant of ingested algae to mussel production, and ν characterizes the rate at which algae is supplied to the mussel bed by the water flow. The mussel mortality is assumed to decrease when mussel density increases because of a reduction of dislodgment and predation in dense clumps. This assumption is represented in the term $k_m/(k_m + M)$, where k_M is the value of M at which mortality is half of the maximal. D is the diffusion rate of the mussels. The diffusion rate of mussels depends on their age. Mussels in young beds diffuse at faster rates than in the mature beds. We refer the reader to [13] for detailed explanation of the deduction of the model and references on which it is based, as well as tables of representative values of the parameters.
In this paper we will consider a one-dimensional version of (1.1),

$$\begin{aligned} A_\tau &= (A_{up} - A)f - \frac{c}{h}AM - \nu A_x, \\ M_\tau &= ecAM - d_M\frac{k_m}{k_m + M}M + DM_{xx}, \end{aligned} \tag{1.2}$$

posed on $(x, \tau) \in \mathbb{R} \times \mathbb{R}^+$. It is known that even for young mussels the values of parameter D are quite small compared to the values of other parameters (about 10^{-3} times smaller) so we think of D as a small parameter no matter whether mussel beds are young or mature.
In [13], van der Kopel and collaborators performed numerical simulations on a non - dimensionalized version of system (1.2), which reads

$$\begin{aligned} a_t &= \tilde{\alpha}(1 - a) - am - \tilde{\beta}a_x, \\ m_t &= \tilde{\delta}am - \tilde{\gamma}\frac{m}{1 + m} + m_{xx}, \end{aligned} \tag{1.3}$$

where the relationships between the new and original quantities are $a = A_{up}^{-1}A$, $m = k_M^{-1}M$, $T = ck_Mh^{-1}$, the space and time are scaled as $x = T^{1/2}D^{-1/2}X$, and $t = T\tau$, and new parameters are $\tilde{\alpha} = fT^{-1}$, $\tilde{\beta} = VD^{-1/2}T^{-1/2}$, $\tilde{\gamma} = d_MT^{-1}$, $\tilde{\delta} = ecA_{up}T^{-1}$. The study in [13] is focused on the relation of pattern formation on the mussel bed with the resilience of mussel bed systems to disturbances. Among other things, the authors demonstrated that self-organized spatial patterns improve the resilience of mussel beds. We refer readers to the original paper for detailed ecological implications of the results obtained in [13]. In a follow-up paper [14] further investigation of periodic patterns in the same system was performed numerically using AUTO [4].The authors also briefly mentioned in Sect. 4 that for certain parameter values monotone or oscillatory traveling waves in the system have been observed in AUTO calculations.
In this paper we present a systematic analytical study of traveling waves in (1.2). We consider a non - dimensionalization of (1.2) that is different from (1.3), as it represents a different time and space scalings as well as a different scaling for M. More precisely, we keep the spacial variable the same as in (1.2) and set $t = ecA_{up}\tau$, then denote $u(x, t) = A(x, t)/A_{up} = a(x, t)$

and $v(x,t) = fhc^{-1}M(x,t)$. The system (1.2) then reads

$$\begin{aligned} u_t &= \frac{f}{ec}(1-u-uv) - \frac{\nu}{ecA_{up}}u_x, \\ v_t &= uv - \frac{d_m}{ecA_{up}}\frac{v}{(1+fh(ck_m)^{-1}v)} + \frac{D}{ecA_{up}}v_{xx}. \end{aligned} \tag{1.4}$$

Using the following notations

$$\delta = f(ec)^{-1},\ \ \alpha = fh(ck_m)^{-1},\ \ \varepsilon = D(A_{up}ec)^{-1},\ \ \beta = \nu(ecA_{up})^{-1},\ \ \gamma = d_m(ecA_{up})^{-1}, \tag{1.5}$$

we then rewrite system (1.4) as

$$u_t = \delta(1-u-uv) - \beta u_x, \tag{1.6}$$

$$v_t = uv - \gamma\frac{v}{1+\alpha v} + \varepsilon v_{xx}. \tag{1.7}$$

This system has one more parameter than in (1.3), but we prefer to keep ε in the system and not scale it out since we want to treat it as a small parameter in our analysis which is based on the Singular Perturbation Theory. In the next section we demonstrate that this scaling produces a form which is convenient for bifurcation analysis of traveling waves.
Traveling waves are solutions of the underlying partial differential equation that preserve their shape while propagating to an infinity. They are important solutions that sometimes arise in partial differential equations posed on infinite domains. If stable, these solutions are observed as coherent structures in the system. If unstable, the type of their instability dictates how solutions that start near the traveling waves behave. There are different types of traveling waves, but in this work are interested in periodic wave trains, traveling waves that asymptotically connect two different constant states, and traveling waves that connect a periodic wave train to a constant state. The former are called fronts, and the latter can be considered a generalization of fronts. Schematically these waves are represented in Fig.1.1.

2. Existence of traveling waves.

We are interested in traveling wave solutions of the coupled system of partial differential equations (1.4). To analyze existence of traveling waves, we consider system (1.4) in a moving coordinate frame $\xi = x - ct$, where c is a parameter that represents the speed of the wave. System (1.4) in the new coordinate frame reads

$$\begin{aligned} u_t &= \delta(1-u-uv) + (c-\beta)u_\xi, \\ v_t &= uv - \frac{\gamma v}{1+\alpha v} + cv_\xi + \varepsilon v_{\xi\xi}. \end{aligned} \tag{2.1}$$

Traveling waves are stationary solutions of this system of partial differential equations. As such, they can be sought as solutions of the following system of ordinary differential equations

$$\begin{aligned} (c-\beta)u_\xi + \delta(1-u-uv) &= 0 \\ \varepsilon v_{\xi\xi} + cv_\xi + uv - \frac{\gamma v}{1+\alpha v} &= 0. \end{aligned} \tag{2.2}$$

FIGURE 1.1. The existence of the following types of waves is shown in this work: a) fronts with monotone tails and fronts with oscillatory tails, b) fronts that connect a periodic wave train to a spatially homogeneous state, c) periodic wave trains.

We note that here different signs of c may lead to solutions of qualitatively different nature. We rescale the spatial variable ξ in the system (2.2) as $\xi = cz$, and introduce our bifurcation parameter η and a new parameter ϵ as

$$\eta = \frac{c\delta}{c-\beta}, \qquad \epsilon = \frac{\varepsilon}{c^2}. \tag{2.3}$$

The traveling wave equations (2.2) then become

$$\begin{aligned} u' + \eta(1-u-uv) &= 0, \\ \epsilon v'' + v' + uv - \frac{\gamma v}{1+\alpha v} &= 0, \end{aligned} \tag{2.4}$$

where the derivative is taken with respect to z. This system can be written as a first order system for $u_1 = u$, $v_1 = v$, and $v_2 = v'$,

$$\begin{aligned} u_1' &= \eta(u_1 v_1 + u_1 - 1), \\ v_1' &= v_2, \\ \epsilon v_2' &= -v_2 + \frac{\gamma v_1}{1+\alpha v_1} - u_1 v_1, \end{aligned} \tag{2.5}$$

or, equivalently, in a coordinate $\zeta = z/\epsilon$,

$$\begin{aligned} \dot{u}_1 &= \epsilon\eta(u_1 v_1 + u_1 - 1), \\ \dot{v}_1 &= \epsilon v_2, \\ \dot{v}_2 &= -v_2 + \frac{\gamma v_1}{1+\alpha v_1} - u_1 v_1, \end{aligned} \tag{2.6}$$

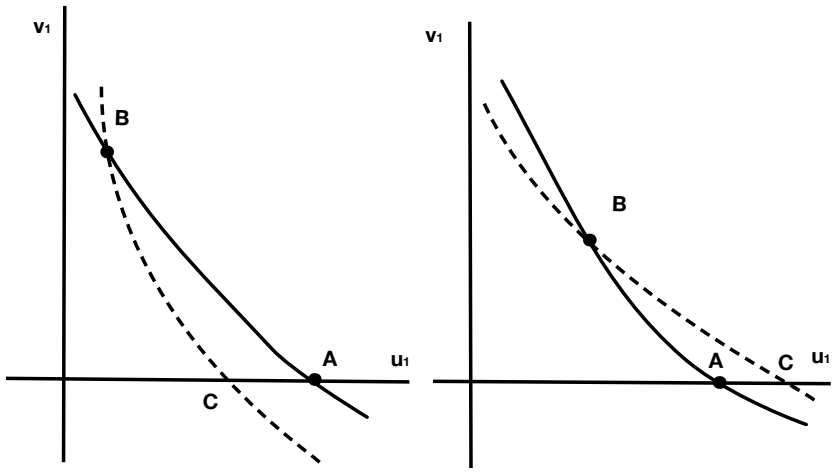

FIGURE 2.1. Nullclines and equilibria on $(u_1, v_1, 0)$-plane: $A = (1, 0, 0)$ and $B = (\frac{\alpha-\gamma}{\alpha-1}, \frac{\gamma-1}{\alpha-\gamma}, 0)$ are the equilibrium points. $C = (\gamma, 0, 0)$ is an auxiliary point. The dashed curve is $\Gamma_3 = \{(\gamma/(1+\alpha v_1), v_1, 0)\}$ and the solid curve t is $\Gamma_1 = \{(1/(1+v_1), v_1, 0)\}$.

where the derivative is taken with respect to ζ. We shall refer to system (2.5) as the slow system and (2.6) as the fast system. These two systems are equivalent when $\epsilon \neq 0$. They have the same equilibria. The point $A = (1, 0, 0)$ is an equilibrium regardless the values of α and γ. When $\gamma = \alpha = 1$, there is a curve of equilibrium points $\Gamma_1 = \{(1/(1+v_1), v_1, 0)\}$ that contains A. When $\gamma = 1$ but $\alpha \neq 1$ and when $\gamma \neq 1$ but $\alpha = \gamma$ the only equilibrium is at A. In the complement to the union of the lines $\gamma = 1$ and $\gamma = \alpha$ there are exactly two distinct equilibria

$$A = (1, 0, 0) \text{ and } B = \left(\frac{\alpha-\gamma}{\alpha-1}, \frac{\gamma-1}{\alpha-\gamma}, 0\right).$$

Due to the physical meaning of the quantities involved, we are interested in parameter regimes that yield nonnegative coordinates of B, and, moreover, in connections between equilibria A and B with always nonnegative u_1 and v_1- components. Therefore, within the complement to $\{\gamma = 1 \cup \gamma = \alpha\}$ in the (γ, α)-plane, we only consider sectors

$$1 < \gamma < \alpha \text{ and } 0 < \alpha < \gamma < 1. \tag{2.7}$$

The equilibrium points $A = (1, 0, 0)$ and B (when α and γ are as in (2.7)) are schematically represented in Fig. 2.1 on $(u_1, v_1, 0)$-plane. The equilibrium A is the intersection of the curve $\Gamma_1 = \{(1/(1+v_1), v_1, 0)\}$ with the curve $\Gamma_2 = \{(u_1, 0, 0)\}$ and the equilibrium B is the intersection of the curve Γ_1 with the curve $\Gamma_3 = \{(\gamma/(1+\alpha v_1), v_1, 0)\}$. The point $C = (\gamma, 0, 0)$ is not an equilibrium, but will be used to describe phenomenologically different cases.

When $\epsilon = 0$, a reduced system can be obtained from (2.5) as follows. The last equation in (2.5) reduces to

$$-v_2 + \frac{\gamma v_1}{1+\alpha v_1} - u_1 v_1 = 0.$$

On this set, the limiting slow equations are

$$\begin{aligned} u_1' &= \eta(u_1 v_1 + u_1 - 1), \\ v_1' &= \frac{\gamma v_1}{1+\alpha v_1} - u_1 v_1. \end{aligned} \tag{2.8}$$

On the other hand, the system (2.6) in the limit $\epsilon \to 0$ is

$$\begin{aligned} u_1' &= 0, \\ v_1' &= 0, \\ v_2' &= -v_2 + \frac{\gamma v_1}{1+\alpha v_1} - u_1 v_1. \end{aligned} \tag{2.9}$$

The set

$$M(0) = \{(u_1, v_1, v_2) : \ v_2 = \frac{\gamma v_1}{1+\alpha v_1} - u_1 v_1\}$$

is a 2-dimensional set of equilibria for (2.9). The linearization of the system (2.9) about any point in this set has two zero eigenvalues and one negative eigenvalue. Therefore $M(0)$ is an invariant, normally hyperbolic, and attracting set for (2.6). Under these conditions invariant manifold theory by Fenichel is applicable. More precisely, by Fenichel's First Theorem ([7], [8]), the critical set $M(0)$, at least over compact sets, perturbs to an invariant set $M(\epsilon)$ for (2.6) with $\epsilon > 0$ but sufficiently small. The distance between $M(0)$ and $M(\epsilon)$ is of order ϵ,

$$M(\epsilon) = \{(u_1, v_1, v_2) : v_2 = \frac{\gamma v_1}{1+\alpha v_1} - u_1 v_1 + \mathrm{O}(\epsilon)\}.$$

If ϵ is small enough, $M(\epsilon)$ is also normally hyperbolic and attracting on the fast scale $\zeta = z/\epsilon$. The slow flow on $M(\epsilon)$ is given by

$$\begin{aligned} \dot{u}_1 &= \epsilon(\eta(v_1 u_1 - 1 + u_1) + \mathrm{O}(\epsilon)), \\ \dot{v}_1 &= \epsilon(\frac{\gamma v_1}{1+\alpha v_1} - u_1 v_1 + \mathrm{O}(\epsilon)). \end{aligned} \tag{2.10}$$

Recall that the reduced flow on the critical manifold is given by (2.8).

In the next few sections we will take a closer look at the flow generated by the reduced system (2.6). The analysis depends on the parameters α, γ and η. Notice that the sign of η is determined by the sign of $c - \beta$, in other words, it is determined by the relation between the speed of the current and the speed of the traveling wave. We find it convenient to divide the 3-dimensional parameter space on the following regions:

(i) Region 1: $1 < \gamma < \alpha$, $\eta < 0$;
(ii) Region 2: $0 < \alpha < \gamma < 1$, $\eta < 0$;
(iii) Region 3: $1 < \gamma < \alpha$, $\eta > 0$;
(iv) Region 4: $0 < \alpha < \gamma < 1$, $\eta \in \left[\frac{\alpha(\gamma-1)(\alpha-\gamma)^2}{(\alpha-1)^3\gamma}; \infty\right)$;

(v) Region 5: $0 < \alpha < \gamma < 1$, $\eta \in \left(0, \frac{\alpha(\gamma-1)(\alpha-\gamma)^2}{(\alpha-1)^3\gamma}\right)$.

In this paper we concentrate on Regions 1, 2, 3, and 4. Region 5 will be studied separately. The plan of the paper is as follows. The analysis of the existence of the heteroclinic orbits in Regions 1 and 2 is significantly different from the analysis in Regions 3 and 4. In Regions 1 and 2 we use "non-traditional" trapping region type argument to prove the existence of the orbits. The argument is based on the fact that for each of these parameter regimes there exists two singular orbits that can serve as boundaries of the trapping region, despite the fact that they do not exists for the same parameters. They are in some sense "invisible" obstacles. We these arguments are presented in Section 3.

In Regions 3 and 4, only one singular orbit exists which is not enough to create a "trapping" enclosure. Nevertheless, we are able to extend a local existence result (the existence of the singular wave in the limiting system) to an interval of values of η which is not small by using a compactification argument. This is done in Section 4.

3. Analysis of the reduced flow, $\eta < 0$.

3.1. **Region 1:** $1 < \gamma < \alpha$, $\eta < 0$.

Theorem 3.1. *For each fixed α, η, γ from Region 1, there exists $\epsilon_0 > 0$ such that for any $\epsilon < \epsilon_0$ there is a heteroclinic orbit that connects a saddle A to a stable node B.*

Remark 3.2. *Existence of a heteroclinic orbit implies that for fixed δ and β and sufficiently small ε there is a front solution that moves with a prescribed speed $c = c(\delta, \beta)$ in (2.2) with ε defined as $\varepsilon = c^2\epsilon$ according to (2.3). Here and throughout the paper when we say "a front" we mean a front together with the family of its translations.*

In this particular parameter regime it is guaranteed that, in the plane $v_2 = 0$, the equilibrium $A = (1, 0, 0)$ in Fig. 3.1 is strictly to the left of the point $C = (\gamma, 0, 0)$.

Consider the reduced system (2.8). The parameter η in this regime is negative, so we denote $|\eta| = \sigma_1$ and write (2.8) as

$$\begin{aligned} u_1' &= -\sigma_1(v_1u_1 - 1 + u_1), \\ v_1' &= \frac{\gamma v_1}{1 + \alpha v_1} - u_1v_1. \end{aligned} \tag{3.1}$$

We will treat this system as one with a multi-scale structure imposed by presence of η. More precisely, we will consider this system with $\sigma_1 \ll 1$ and, separately, with $\sigma_1 \gg 1$. In the latter case, we use $\sigma_2 = 1/\sigma_1$ as the singular parameter.

When $\sigma_1 \ll 1$, this system is a singular perturbation of

$$\begin{aligned} u_1' &= 0, \\ v_1' &= \frac{\gamma v_1}{1 + \alpha v_1} - u_1v_1. \end{aligned} \tag{3.2}$$

The sets

$$L_1(\sigma_1 = 0) = \{(u_1, v_1), v_1 = 0\} \tag{3.3}$$

and

$$L_2(\sigma_1 = 0) = \{(u_1, v_1), v_1 = \frac{\gamma - u_1}{\alpha u_1}\} \tag{3.4}$$

are lines of equilibria for the fast system (3.2). For each $u_1 = u_1^* < \gamma$, the equilibrium $(u_1^*, 0)$ of (3.2) has a one-dimensional central manifold and a one-dimensional unstable manifold (corresponding to the positive eigenvalue $\gamma - u_1^*$. On the other hand, for each $u_1 = u_1^* < \gamma$, the equilibrium $(u_1^*, \frac{\gamma - u_1^*}{\alpha u_1^*})$ that belongs to $L_2(\sigma_1 = 0)$ has a one-dimensional central manifold and a one-dimensional stable manifold. The portion of the curve $L_2(\sigma_1 = 0)$ that corresponds to $u_1 < \gamma$ has then a two-dimensional stable manifold which intersects with a one-dimensional unstable manifold of each $(u_1^*, 0)$ transversally (by dimension counting). Therefore, for each fixed $u_1 = u_1^*$, there is a fast connection that connects $(u_1^*, 0)$ to the point $(u_1^*, \frac{\gamma - u_1^*}{\alpha u_1^*}) \in L_2(\sigma_1 = 0)$.

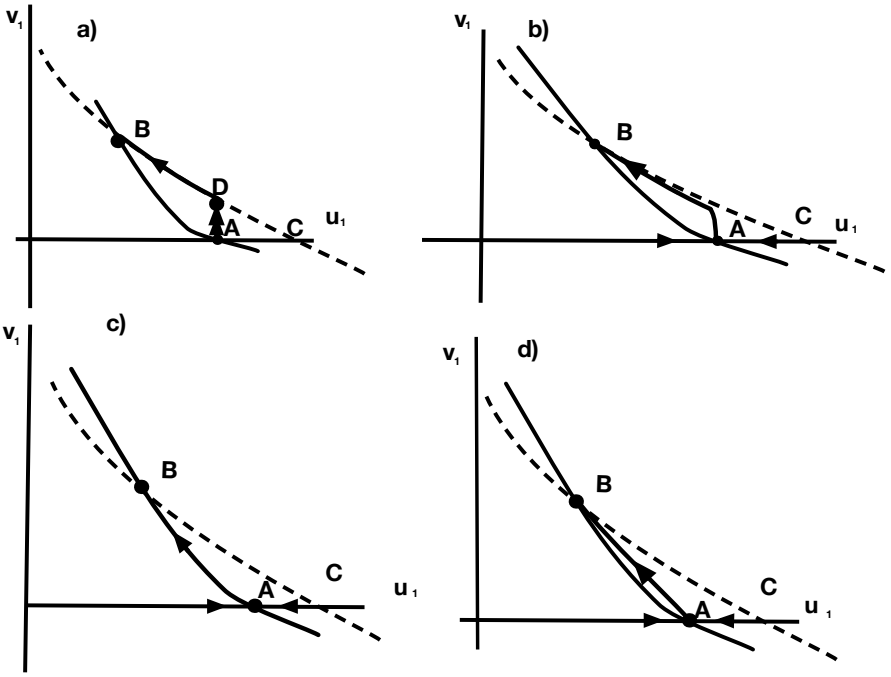

FIGURE 3.1. Region 1: a) Singular wave, $\sigma_1 = 0$. b) Wave in the perturbed system, $\sigma_1 \ll 1$. c) Singular wave, $\sigma_2 = 0$. b) Wave in the perturbed system, $\sigma_2 \ll 1$.

The slow flow on the set $L_2(\sigma_1 = 0)$ is given by

$$\dot{u}_1 = -(1 - \frac{1}{\alpha})u_1 - \frac{\gamma}{\alpha} + 1. \tag{3.5}$$

Equation (3.5) has one stable (since $\alpha > 1$) equilibrium that corresponds to equilibrium B of the full system. There is then a singular orbit between A and B that consists of two pieces:

a fast piece that connects the equilibrium $A = (1, 0, 0)$ to the point $D = (1, \frac{\gamma-1}{\alpha}, 0)$ that belongs to $L_2(\sigma_1 = 0)$ and a slow piece that connects D to the equilibrium A. See Fig. 3.1, panel a) for the illustration.

Because of the transversality of the intersection, this orbit persists upon switching on $\sigma_1 \ll 1$ (see Fig. 3.1, panel b)). More precisely, there exists a $\tilde{\sigma}_1$ such that for any $0 < \sigma_1 \leq \tilde{\sigma}_1$ there exits a heteroclinic orbit.

Moreover for fixed parameters σ_1, γ, and α there is an ϵ_0 small enough such that for each $\epsilon < \epsilon_0$ this orbit persists as a solution of the full system (2.5) which connects the saddle at A to the stable stable equilibrium B as implied by the Geometric Singular Perturbation Theory [7] or [8].

Next we consider the singular limit $\sigma_2 = 1/\sigma_1 \ll 1$. The system (3.1) is then singularly perturbed with the small parameter σ_2. After rescaling the system (2.8) reads

$$\begin{aligned} u_1' &= -(v_1 u_1 - 1 + u_1), \\ v_1' &= \sigma_2(\tfrac{\gamma v_1}{1+\alpha v_1} - u_1 v_1). \end{aligned} \tag{3.6}$$

We note that we use the same notation for the derivatives here and in the systems above which are taken with respect to the appropriate, different coordinates.

We let $\sigma_2 \to 0$ and obtain the fast reduced system

$$\begin{aligned} u_1' &= -(v_1 u_1 - 1 + u_1), \\ v_1' &= 0. \end{aligned} \tag{3.7}$$

The set $L_3(\sigma_2 = 0) = \{(u_1, v_1), u_1 = \frac{1}{v_1+1}\}$ is a line of equilibria for the limiting system (3.7). The slow flow on $L_3(\sigma_2 = 0)$ is given by

$$\dot{v}_1 = \frac{\gamma v_1}{1 + \alpha v_1} - \frac{v_1}{v_1 + 1}.$$

The set $L_3^+(\sigma_2 = 0) = \{(u_1, v_1), u_1 = \frac{1}{v_1+1}, v_1 > 0\}$ is normally hyperbolic, and attracting invariant set for (3.7). Indeed, linearization of (3.7) around each equilibria $(\frac{1}{v_1^*+1}, v_1^*)$ has a zero eigenvalue and an eigenvalue $-1 - v_1^*$. Under small perturbations it persists as an invariant manifold $L_3(\sigma_2)^+$ for (3.7). The slow flow on the perturbed normally hyperbolic invariant set $L_3(\sigma_2)^+$ is given by

$$\dot{v}_1 = \frac{v_1(v_1(\gamma - \alpha) - 1 + \gamma)}{(1 + \alpha v_1)(v_1 + 1)} + O(\sigma_2). \tag{3.8}$$

This equation of first order possesses one unstable equilibrium that corresponds to the saddle equilibrium A and one stable equilibrium that corresponds to the equilibrium B and a solution that connects them. The unstable equilibrium corresponds to equilibrium B of the full system and the stable equilibrium corresponds to the equilibrium A of the full system. The solution that connects equilibria of (3.8) corresponds to the heteroclinic orbit of (3.1) that connects A to B which is near $L_3(\sigma_2 = 0)$. More precisely, there exists a $\tilde{\sigma}_2$ such that

for any $\sigma_2 \leq \tilde{\sigma}_2$ (alternatively, $\sigma_1 \geq \tilde{\tilde{\sigma}}_1 = 1/\tilde{\sigma}_2$) there exits an orbit that asymptotically connects A to B (see 3.1 b)).

Dimension counting shows that this orbit persists as a solution of the full system when is $\epsilon \ll 1$ as implied by the Geometric Singular Perturbation Theory.

Existence of traveling waves at and near limits when $\sigma_1 = |\eta| \to 0$ and $\sigma_2 = 1/\sigma_1 \to 0$ are local results - they hold for sufficiently small and sufficiently large values of σ_1. The existence of the waves for every σ_1 follows from the theory of rotation vector fields [5], [11] and a "trapping region" type argument.

We think of (3.1) (or, alternatively, (3.6)) as a two-dimensional dynamical system with planar vector field generated by $F = (f_1, f_2)$, where $f_1(u_1, v_1) = -\sigma_1(v_1 u_1 - 1 + u_1)$ and $f_2(u_1, v_1) = \frac{\gamma v_1}{1+\alpha v_1} - u_1 v_1$. Note that the nullclines of this system (and, therefore, the equilibria themselves) are independent of the parameter σ_1. Denote the angle between the u_1-axis and the vector $F(u_1, u_2)$ by

$$\theta(u_1, v_1) = \tan^{-1} \frac{f_2(u_1, v_1)}{f_1(u_1, v_1)}.$$

At each point (u_1, v_1), $\frac{\partial \theta}{\partial \sigma_1}$ measures the rate of change of θ as a function of σ_1. In our case,

$$\frac{\partial \theta}{\partial \sigma_1} = \frac{f_1 \frac{\partial f_2}{\partial \sigma_1} - f_2 \frac{\partial f_1}{\partial \sigma_1}}{f_1^2 + f_2^2} = -\frac{v_1(1+v_1)\left(u_1 - \frac{1}{1+v_1}\right)\left(u_1 - \frac{\gamma}{1+\alpha v_1}\right)}{\sigma_1^2(u_1(v_1+1)-1)^2 + \left(\frac{\gamma}{1+\alpha v_1} - u_1\right)^2 v_1^2} \tag{3.9}$$

is positive in the region bounded by the nullclines and the u_1-axis. So as σ_1 increases the vector field in that region rotates counterclockwise. The system (3.1) (and, similarly, (3.6)) defines a rotating vector field [5], [11]. This, in part, implies that the waves in both singular limit cases $\sigma_1 = 0$ and $\sigma_1 = \infty$ ($\sigma_2 = 0$) perturb to waves that entirely belong to the region bounded by the nullclines and the u_1-axis.

We consider (3.1) with fixed values of parameters γ and α. Let σ_1 be a value $\tilde{\sigma}_1 < \sigma_1 < \tilde{\tilde{\sigma}}_1$. The stable manifold $W^u(A)(\sigma_1)$ of the equilibrium A is then located between the stable manifolds of A with $\tilde{\sigma}_1$ and $\tilde{\tilde{\sigma}}_1$. It was proved in [11, Section 2, Precession of Saddle Separatrices] that, as σ_1 increases within interval $[\tilde{\sigma}_1, \tilde{\tilde{\sigma}}_1]$, the saddle separatrices (here solutions that follow $W^s(A)(\sigma_1)$) (a) move monotonically counterclockwise along transversals (i.e. along each sufficiently small circle centered at the saddle point A) from the initial position to the final position which is the orbit that corresponds to $\tilde{\tilde{\sigma}}_1$; (b) never self-intersect, i.e. $W^s(A)(\sigma_1^*) \cap W^s(A)(\sigma_1^{**}) = \emptyset$, for $\sigma_1^* \neq \sigma_1^{**}$. Therefore the orbit that follows $W^s(A)(\sigma_1)$ for any $\sigma_1 \in [\tilde{\sigma}_1, \tilde{\tilde{\sigma}}_1]$ will have to enter the only other equilibrium in that region, equilibrium B, thus creating a heteroclinic orbit. This completes the proof of the existence of the traveling waves for the Region 1.

The argument used above can be viewed as non-traditional "trapping region" type argument, since the boundaries of the region (orbits for $\tilde{\sigma}_1$ and $\tilde{\tilde{\sigma}}_1$) exist not for the same parameters as

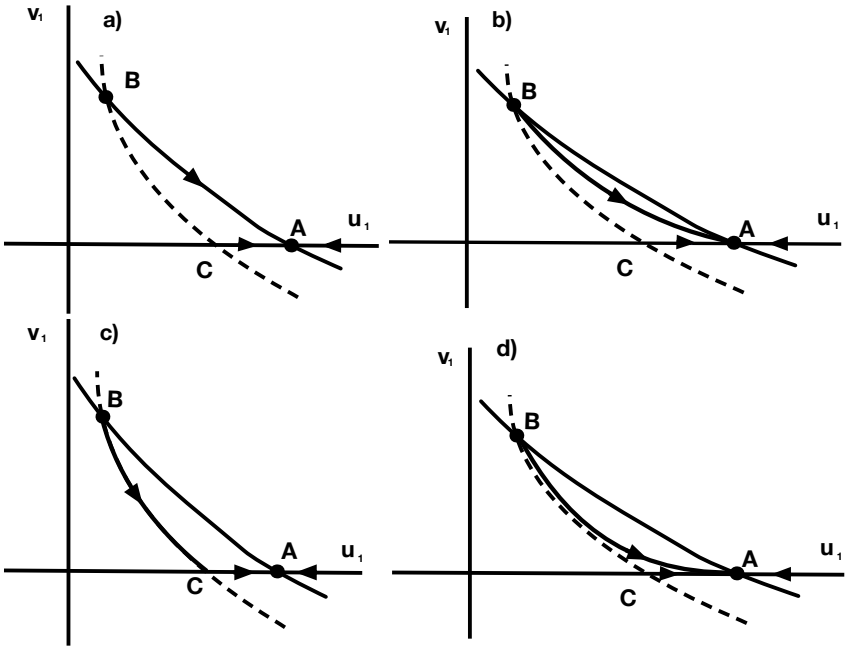

FIGURE 3.2. When parameters belong to Region 2, A is an attractor and B is a saddle. The unstable manifold of B rotates between the two singular positions.

the solution that is considered (some fixed $\sigma_1 \in [\tilde{\sigma}_1, \tilde{\tilde{\sigma}}_1]$) but nevertheless serve as obstruction for the solution that does not allow it to leave the region.

3.2. **Region 2:** $0 < \alpha < \gamma < 1$**,** $\eta < 0$**.**

Theorem 3.3. *For each fixed α, η, γ from Region 2, there exists ϵ_0 such that for any $\epsilon < \epsilon_0$ there is a heteroclinic orbit that asymptotically connects B to A.*

In this parameter regime the equilibrium $A = (1, 0, 0)$ is strictly to the right of the point $C = (\gamma, 0, 0)$ on the plane $v_2 = 0$ (see Fig. 3.2).
Recall that we consider the reduced system (3.1)

$$\begin{aligned} u_1' &= -\sigma_1(v_1 u_1 - 1 + u_1), \\ v_1' &= \frac{\gamma v_1}{1 + \alpha v_1} - u_1 v_1, \end{aligned}$$

where $\sigma_1 = |\eta|$. In the limit $\sigma_1 \to 0$ this system becomes (3.2) which reads

$$\begin{aligned} u_1' &= 0, \\ v_1' &= \frac{\gamma v_1}{1 + \alpha v_1} - u_1 v_1. \end{aligned}$$

The limiting system has two curves of equilibria: $L_2(\sigma_1 = 0) = \{u_1, v_1), v_1 = \frac{\gamma - u_1}{\alpha u_1}\}$ and $L_1(\sigma_1 = 0) = \{u_1, v_1), v_1 = 0\}$. If we linearize the limiting system around each of these

equilibria, we see that the portions of $L_1(\sigma_1 = 0)$ and $L_2(\sigma_1 = 0)$ that we are interested in have useful properties: $L_1^{\rm R}(\sigma_1 = 0) = \{u_1, v_1), v_1 = 0, u_1 < \gamma\}$ is normally repelling, while $L_2^{\rm R}(\sigma_1 = 0) = \{u_1, v_1), v_1 = 0, u_1 > \gamma\}$ and $L_2^{+}(\sigma_1 = 0) = \{u_1, v_1), v_1 = \frac{\gamma - u_1}{\alpha u_1}, v_1 > 0\}$ are normally attracting. The equilibrium at B is a saddle and has a one-dimensional unstable manifold $W^u(B)$. On the other hand, A has two-dimensional stable manifold and is a stable node. The solution that leaves B does so along $W^u(B)$ which happens to be the nullcline $L_2(\sigma_1 = 0)$ and after reaching point C switches to follow the line $v_1 = 0$ which is an invariant set for both (3.1) and the limiting system (3.2).

There exists then a singular heteroclinic orbit that connects B to A. It consists of two slow pieces: a piece that is the segment of L_2^+ that connects B to C and the second piece which is the segment of $L_1^{\rm R}$ that connects C to B. Note that $L_1^{\rm R}$ is an invariant set for (3.1) too. The rotation of the saddle separatrix of B then implies the existence of the heteroclinic orbit that connects B to A in (3.1). More details will follow after the discussion of the second singular wave. By the Geometric Singular Perturbation Theory, when σ_1 is sufficiently small, that heteroclinic orbit is near the singular orbit (see Fig. 3.2).

Next we consider the reduced system (3.6)

$$\begin{aligned} u_1' &= -(v_1 u_1 - 1 + u_1) \\ v_1' &= \sigma_2 (\frac{\gamma v_1}{1 + \alpha v_1} - u_1 v_1) \end{aligned}$$

which is in a fast-slow form with a small parameter $\sigma_2 = 1/|\eta| \ll 1$. The system (3.6) in the limit $\sigma_2 \to 0$,

$$\begin{aligned} u_1' &= -(v_1 u_1 - 1 + u_1), \\ v_1' &= 0, \end{aligned} \tag{3.10}$$

has a curve of equilibria $\{(u_1, v_1),\ u_1 = \frac{1}{v_1 + 1}\}$. Linearization of (3.10) around each of these equilibria, say $(\frac{1}{v_1^* + 1}, v_1^*)$, has a zero eigenvalue and, for $v_1^* > 0$, a negative eigenvalue equal to $-(v_1^* + 1)$. Therefore, the set of equilibria is normally hyperbolic and attracting. By the Geometric Singular Perturbation Theory, it persists as an invariant set for the system (3.6) for sufficiently small σ_2. The reduced flow on the perturbed normally hyperbolic manifold $\{(u, v), v_1 = \frac{1}{v_1 + 1} + O(\sigma_2)\}$ is given by

$$\dot{v}_1 = \frac{v_1 (v_1 (\gamma - \alpha) - 1 + \gamma)}{(1 + \alpha v_1)(v_1 + 1)} + O(\sigma_2). \tag{3.11}$$

It possesses a connection between $v_1 = \frac{\gamma - 1}{\alpha - \gamma}$, which corresponds to the saddle equilibrium B of the full system, and $v_1 = 0$, which corresponds to stable equilibrium A. This solution persists upon switching on the parameter σ_2.

The same way as in Sect. 3.1, for ϵ sufficiently small both singular orbits perturb to heteroclinic orbits for the full system (2.4).

The same argument as in Sect. 3.1, also shows that the heteroclinic orbit between the two fixed points B and A rotates monotonically counterclockwise around the saddle equilibrium at B when $\sigma_1 = |\eta|$ changes from 0 to ∞, because according to formula (3.9), $\frac{\partial\theta}{\partial\sigma_1}$ is positive in Region 2. Therefore both of the perturbed by small $\sigma_1 \leq \tilde{\sigma}_1$ and small $\sigma_2 = 1/\sigma_1$ ($\sigma_1 \geq \tilde{\tilde{\sigma}}_1$) waves entirely belong to the region bounded by the nullclines and the v_1 -axis, and the solution for any $\sigma_1 \in (\tilde{\sigma}_1, \tilde{\tilde{\sigma}})$ that leaves the equilibrium at B is trapped by these two solutions and therefore has to converge to the equilibrium at A.

4. Analysis of the reduced flow, $\eta > 0$.

4.1. **Region 3:** $1 < \gamma < \alpha$, $\eta > 0$.

Theorem 4.1. *For each fixed α, η, γ from Region 3, there exists $\epsilon_0 > 0$ such that for any $\epsilon < \epsilon_0$ there is a front solution that connects a saddle B to an unstable node A.*

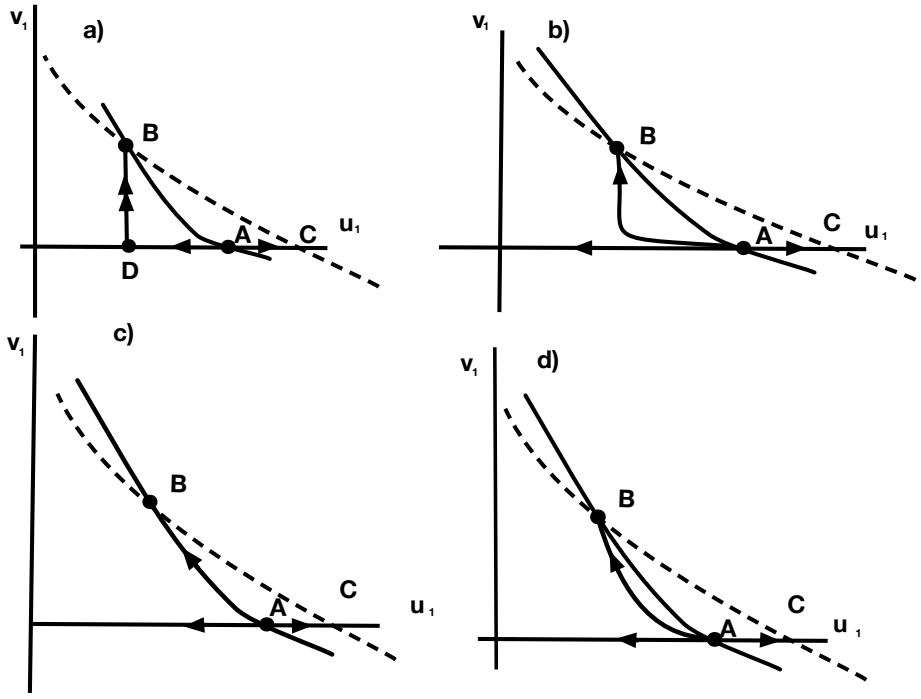

FIGURE 4.1. Region 3: A is a repeller, B is a saddle. a) Singular wave, $\eta = 0$. b) Wave in the perturbed system, $\eta \ll 1$. c) Singular wave, $1/\eta = 0$. b) Wave in the perturbed system, $1/\eta \ll 1$.

The analysis of the heteroclinic orbits connecting A and B in the Region 3 is similar to the analysis of the heteroclinic orbits in Region 1. The construction of the first singular wave does not depend on the sign of η as η is set to zero. When η is sufficiently small the equilibria are of the nature different from ones they have in Region 1: the equilibrium at A is now an unstable node (it was a saddle in Region 1), and the equilibrium at B is a saddle (B was

a stable node in Region 1). The construction of the second limiting wave at $\eta \to \infty$ is also analogous. When η is sufficiently small and sufficiently large, the perturbed waves exists and can be used as boundaries of the "trapping" region. Using calculations similar to (3.9) for Region 4 it is easy to sea that the separatrix of the saddle (here, B) rotates clockwise, therefore the same argument as in Section. 3.1 implies existence of the heteroclinic orbit for any $\eta > 0$. That connection persists as a sufficiently small ϵ is introduced in the problem (see equations (2.5)). Since all of the arguments are essentially similar to ones presented in Sect. 3.1, we omit the details and illustrate the situation in Fig. 4.1.

4.2. **Region 4:** $0 < \alpha < \gamma < 1$, $\eta \in \left[\frac{\alpha(\gamma-1)(\alpha-\gamma)^2}{(\alpha-1)^3\gamma}, \infty\right)$**.** The situation in Region 4 is complex. Below we list the results which hold in different subregions of it. In all of these cases equilibrium A is a saddle node, but they differ by the nature of the equilibrium B.
(i) Region 4A: $\eta \in \left(\frac{(-\alpha+2\gamma+2\sqrt{\gamma(\gamma-\alpha)})(\alpha-\gamma)^2(\gamma-1)}{(\alpha-1)^3\gamma}, \infty\right)$;

Theorem 4.2. *For any α, η, γ from Region 4A there exists $\epsilon_0 > 0$ such that for any $\epsilon < \epsilon_0$, there is an orbit of* (2.5) *that connects the unstable node at B to the saddle at A.*

(ii) Region 4B: $0 < \alpha < \gamma < 1$, $\eta \in \left(\frac{\alpha(\gamma-1)(\alpha-\gamma)^2}{(\alpha-1)^3\gamma}, \frac{(-\alpha+2\gamma+2\sqrt{\gamma(\gamma-\alpha)})(\alpha-\gamma)^2(\gamma-1)}{(\alpha-1)^3\gamma}\right)$;

Theorem 4.3. *For any α, η, γ from Region 4B there exists $\epsilon_0 > 0$ such that for any $\epsilon < \epsilon_0$, there is an orbit of* (2.5) *that connects the unstable focus at B to the saddle at A.*

(iii) In additon, for Region 4C: $\eta = \eta_H = \frac{\alpha(\gamma-1)(\alpha-\gamma)^2}{(\alpha-1)^3\gamma}$, $0 < \alpha < \gamma < 1$, α is sufficiently small, the following result holds.

Theorem 4.4. *There is $0 < \alpha_0 < 1$ such that for any fixed $\alpha < \alpha_0$ and η, γ from Region 4C there exists $\epsilon_0 > 0$ such that for any $\epsilon < \epsilon_0$, in of* (2.5) *the equilibrium B undergoes a subcritical Hopf bifurcation at η_H. Moreover, for $\eta = \eta_H - h$, $0 < h \ll 1$, there exist i) a periodic orbit around the equilibrium B, ii) a heteroclinic orbit of* (2.5) *that asymptotically connects the periodic orbit around B with the equilibrium at A, iii) a manifold of heteroclinic orbits that asymptotically connect the equilibrium at B with the periodic orbit around B.*

The proof of these results uses the analysis of the behavior of the reduced system (2.8) near infinity using Poincaré compactification and Poincaré-Bendixon theorem.
The analysis of the heteroclinic orbits in Regions 4A and 4B is significantly different from the analysis in Regions 1 and 2. While in Regions 1 and 2 the existence of the two limiting waves (for $|\eta| \to 0$ and for $|\eta| \to \infty$) provided us with "trapping regions" for the orbits, in Regions 4A and 4B we are dealing with only one singular wave at $\sigma_3 = 1/\eta$. Nevertheless, we are able to show that an orbit exists for any η as described above. In order to do that we use the compactification and the rotating vector field argument to continue the singular orbit as parameter η changes. To prove Theorems 4.2 and 4.3 we first construct a singular orbit for the limit of the system (2.8) at $\eta \to \infty$. After that we use the Geometric Singular

Perturbation Theory to demonstrate that for sufficiently large η there is a wave in the full equation that is a small perturbation of the limiting wave. In the last part of the proof we use compactification to show that the local in η near ∞ result obtained by the Geometric Singular Perturbation Theory extends to $(\mathcal{H}, \infty)$, where $\mathcal{H}$ is

$$\mathcal{H} = \frac{(-\alpha + 2\gamma + 2\sqrt{\gamma(\gamma-\alpha)})(\alpha-\gamma)^2(\gamma-1)}{(\alpha-1)^3\gamma}. \tag{4.1}$$

Notice that $\mathcal{H} > 0$ when $0 < \alpha < \gamma < 1$. Recall that we are working with the system (2.8) that reads

$$\begin{aligned} u_1' &= \eta(v_1u_1 - 1 + u_1), \\ v_1' &= \frac{\gamma v_1}{1+\alpha v_1} - u_1v_1. \end{aligned}$$

When η is large, this system is singularly perturbed with small parameter $\sigma_3 = 1/\eta$ and can be written as

$$\begin{aligned} \sigma_3 u_1' &= (v_1u_1 - 1 + u_1), \\ v_1' &= \frac{\gamma v_1}{1+\alpha v_1} - u_1v_1, \end{aligned} \tag{4.2}$$

which after rescaling becomes

$$\begin{aligned} u_1' &= v_1u_1 - 1 + u_1, \\ v_1' &= \sigma_3(\frac{\gamma v_1}{1+\alpha v_1} - u_1v_1). \end{aligned} \tag{4.3}$$

In the limit of $\sigma_3 \to 0$ ($\eta \to \infty$) the system reads

$$\begin{aligned} u_1' &= v_1u_1 - 1 + u_1, \\ v_1' &= 0. \end{aligned} \tag{4.4}$$

The set of equilibria of this system is $S(\sigma_3 = 0) = \{(u_1, v_1) : u_1 = \frac{1}{v_1+1}\}$. The linearization of (4.4) around each of these equilibria, say $(\frac{1}{v_1^*+1}, v_1^*)$, has a zero eigenvalue and a positive for $v_1^* > 0$ eigenvalue $1 + v_1^*$. So $S(\sigma_3 = 0)$ is normally hyperbolic and repelling. By the Geometric Singular Theory it persists as an invariant set for the system (4.3) for sufficiently small σ_2. The reduced flow on the perturbed normally hyperbolic invariant set

$$S(\sigma_3) = \{(u_1, v_1), \quad u_1 = \frac{1}{1+v_1} + O(\sigma_3)\}$$

is given by

$$v_1' = \frac{v_1(v_1(\gamma-\alpha) + \gamma - 1)}{(1+v_1)(1+\alpha v_1)} + O(\sigma_3). \tag{4.5}$$

The flow has two equilibria, $v_1 = 0$ and $v_1 = \frac{1-\gamma}{\gamma-\alpha}$ and a connection from $v_1 = \frac{1-\gamma}{\gamma-\alpha}$ to $v_1 = 0$. Dimension counting implies that this connection persists as a solution of (4.2) which corresponds to the heteroclinic orbit of the full system that connects B to A, as it is formed

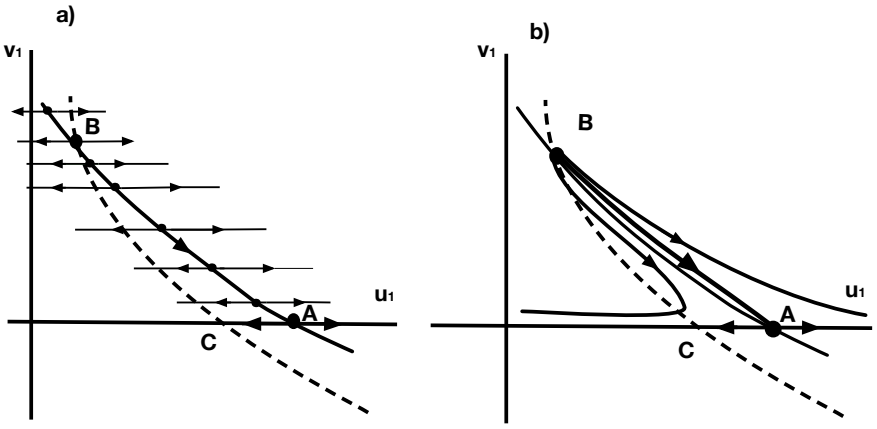

FIGURE 4.2. The left panel schematically represents the singular orbit. On the right, the perturbation of the singular orbit by small σ_3 is illustrated.

as a transversal intersection of the two-dimensional unstable manifold of B with a one-dimensional stable manifold of A in $\mathbb{R}^2$. In other words, there exists $\tilde{\sigma}_3 > 0$ such that for any $\tilde{\sigma}_3 < \sigma_3$ there exists an orbit (see Fig. 4.2) that asymptotically connects B to A which is a perturbation of order $O(\sigma_3)$ of the singular wave.

Since $\sigma_3 = 1/\eta$, next we want to show that as we decrease η further, a topologically equivalent wave (see Fig. 4.3) that connects B to A exists in (4.2) which is a continuous deformation of the singular wave constructed above.

On the other hand, the occurrence of a subcritical Hopf bifurcation follows from the classic Hopf Bifurcation Theorem (see for example, [1, pp. 261-264], or [11, 352]). To claim the conclusion of Theorem 4.4 for system (2.8), one needs to calculate the Lyapunov number. Recall (see [1, p.253]) that for a planar vector field defined by an analytic system,

$$\begin{aligned} \dot{x} &= ax + by + p(x, y), \\ \dot{y} &= cx + dy + q(x, y), \end{aligned}$$

with

$$\Delta = ad - bc > 0, \quad a + d = 0, \quad p(x, y) = \sum_{j+j\geq 2} a_{ij} x^i y^j, \quad q(x, y) = \sum_{j+j\geq 2} b_{ij} x^i y^j,$$

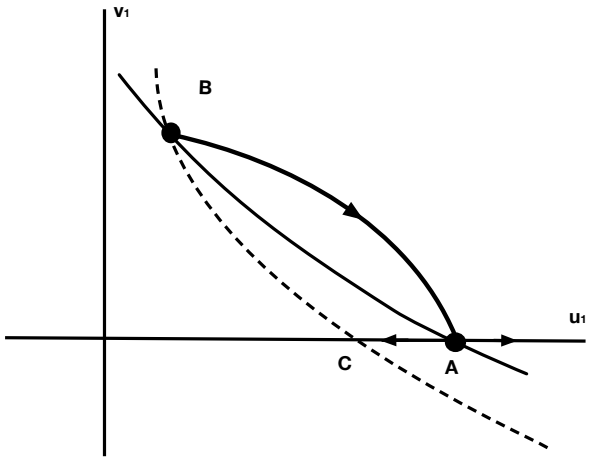

FIGURE 4.3. The heteroclinic orbit persist as σ_3 increases further.

the Lyapunov number is given by the formula

$$\begin{aligned}\sigma = \quad & \frac{-3\pi}{2b\Delta^{3/2}}\{[ac(a_{11}^2 + a_{11}b_{02} + a_{02}b_{11}) + ab(b_{11}^2 + a_{20}b_{11} + a_{11}b_{02}) + c^2(a_{11}a_{02} + 2a_{02}b_{02}) \\ & -2ac(b_{02}^2 - a_{20}a_{02} - 2ab(a_{20}^2 - b_{20}b_{02}) - b^2(2a_{20}b_{20} + b_{11}b_{20} + (bc - 2a^2)(b_{11}b_{02}) \\ & -a_{11}a_{20})] - (a^2 + bc)[3(cb_{03} - ba_{30}) + 2a(a_{21} + b_{12}) + (ca_{12} - bb_{21})]\}.\end{aligned}$$

To perform this calculation in our case, we first notice that on the closed upper half-plane $\{(u_1, v_1),\ v_1 \geq 0\}$, the system (2.8) is topologically equivalent to

$$\begin{aligned} u_1' &= \eta(\alpha v_1 + 1)(v_1 u_1 - 1 + u_1), \\ v_1' &= v_1(\gamma - u_1(1 + \alpha v_1)), \end{aligned} \tag{4.6}$$

via coordinate transformation

$$\zeta = \int_0^{\xi} \frac{1}{1 + \alpha v_1}\, ds.$$

As before, with an abuse of notation, we use $'$ to denote the derivative with respect the new variable ξ. It is also clear that the equilibrium of (2.8) can be shifted to origin by a linear transformation. The new system generates a polynomial vector field. The formula for the Lyapunov number σ is applicable. It yields a not so inconvenient for the analysis expression, $\sigma = \frac{\pi}{P(\alpha,\gamma)} G(\alpha, \gamma)$, where

$$P(\alpha, \gamma) = 1.5\gamma(1 - \alpha)(1 - \gamma)(\gamma - \alpha)^2\sqrt{\alpha(\gamma - \alpha)},$$

and

$$\begin{aligned} G(\alpha, \gamma) = \quad & -\alpha^6 + (2\gamma + 1)\alpha^5 + (\gamma^2 - 2\gamma - 3)\alpha^4 \\ & -(2\gamma^3 + 3\gamma^2 - 6\gamma - 3)\alpha^3 + (\gamma^4 + 3\gamma^2 - 6\gamma - 1)\alpha^2 + (2\gamma - \gamma^2)\alpha. \end{aligned}$$

We note that $P(\alpha,\gamma) > 0$ within this regime, $G(0,\gamma) = 0$, and $\frac{\partial G}{\partial \alpha}(0,\gamma) = \gamma(2-\gamma) > 0$ when $0 < \gamma < 1$. Therefore, for sufficiently small α, σ is positive. Thus the equilibrium B is nonlinearly unstable when $\eta = \eta_H$ and, as η passes through η_H, B generates an unstable limit cycle, thus B undergoes a subcritical Hopf bifurcation. This concludes the proof of Theorem 4.4. The existence of an orbit that connects a closed orbit around B to the equilibrium A follows from the Poincaré-Bendixon theorem and the compactification.
Unlike the previous cases, Regime 1 and Regime 2, here we have only one limiting, singular wave and we do not have a trapping region to use for the analysis. Nevertheless, calculation of the eigenvector corresponding to the stable direction at A shows that the one-dimensional stable manifold of A as it follows its tangent vector $(-1, 1+(1-\eta)\eta^{-1}))$ rotates clockwise as η decreases and therefore leaves the nullcline by going to the right of it. Further, formula (3.9) shows that the direction of rotation is preserved as η decreases from ∞ to 0. To study the behavior of the trajectory that leaves the equilibrium A, we use the Poincaré compactification procedure. The goal is to show that the heteroclinic connection from B to A is structurally stable and is preserved as η is varied over a large interval. The Poincaré compactification procedure involves projecting the Poincaré sphere $S^2 = \{(X,Y,Z) \in \mathbb{R}^3,\ X^2+Y^2+Z^2 = 1\}$ onto (u_1, v_1)-plane tangent to S^2 at the north pole. It is described in detail in the next section.

4.3. **Compactification.** In this section instead of (2.8) we continue to work with the topologically equivalent on $\{(u_1, v_1),\ v_1 \geq 0\}$ system (4.6). To map the upper hemisphere of the Poincaré sphere $\mathbb{S}^2$ onto the (u_1, v_1)-plane, one introduces a coordinate transformation $u_1 = X/Z$, $v_1 = Y/Z$. Then

$$X = \frac{u_1}{\sqrt{1+u_1^2+v_1^2}}, \quad Y = \frac{v_1}{\sqrt{1+u_1^2+v_1^2}}, \quad Z = \frac{1}{\sqrt{1+u_1^2+v_1^2}}. \tag{4.7}$$

The points on the equator $X^2+Y^2 = 1$ on the Poincaré sphere correspond to the infinity of the (u_1, v_1)-plane. Since

$$du_1 = \frac{ZdX - XdZ}{Z^2}, \quad dv_1 = \frac{ZdY - YdZ}{Z^2},$$

the induced flow on the Poincaré sphere is given by the following differential form [2, 12]:

$$Zf_2(\frac{X}{Z},\frac{Y}{Z})dX - Zf_1(\frac{X}{Z},\frac{Y}{Z})dY + (Yf_1(\frac{X}{Z},\frac{Y}{Z}) - Xf_2(\frac{X}{Z},\frac{Y}{Z}))dZ = 0, \tag{4.8}$$

where

$$\begin{aligned} f_1(u_1,v_1) &= \eta(\alpha v_1+1)(-1+u_1+u_1v_1), \\ f_2(u_1,v_1) &= v_1(\gamma - u_1(1+\alpha v_1)). \end{aligned}$$

We desingularize (4.8) and look for the critical points on the equator of the Poincaré sphere. These critical points correspond to critical points of the original system at infinity and can

be found by setting $Z = 0$ in the desingularized version of (4.8), which then reads

$$-\alpha Y^2 X(Y\eta + X) = 0. \tag{4.9}$$

We solve this equation under the conditions $X^2 + Y^2 = 1$ and $Y \geq 0$ and obtain four critical points $E_1 = (-1, 0)$, $E_2 = (-\eta/\sqrt{1+\eta^2}), 1/\sqrt{1+\eta^2})$, $E_3 = (0, 1)$, and $E_4 = (1, 0)$. We are interested in the flow near the critical points at infinity. According to [3] the flow on the equator in polar coordinates is given by the first order differential equation

$$\dot{\theta} = -\alpha \sin^2(\theta)\cos(\theta)(\sigma \sin(\theta) + \cos(\theta)). \tag{4.10}$$

The flow on the upper-half plane is schematically shown on Fig. 4.4. Since the degree of the polynomial vector field, which is the maximum of the degrees of the polynomials $f_1(u_1, v_1)$ and $f_2(u_1, v_1)$, is 3 (an odd number), the antipodal critical points at infinity are qualitatively equivalent [6, 2]. We carry out the analysis of equilibria at infinity by considering the flow on three local charts of the Poincaré sphere:

$$U_y^+ = \{(x, y, z) \in \mathbb{S}^2 | y > 0\}, \quad U_x^+ = \{(x, y, z) \in \mathbb{S}^2 | x > 0\}, \quad U_x^- = \{(x, y, z) \in \mathbb{S}^2 | x < 0\}.$$

Using the third chart U_x^- makes it easier to determine the flow on the upper half-plane near the degenerate equilibrium at the intersection of the equator and the x-axis.

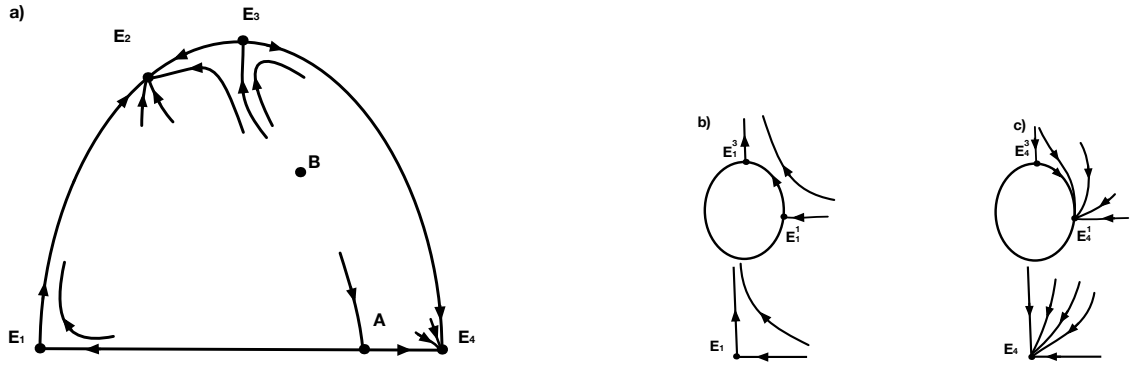

FIGURE 4.4. a) The flow on the equator and near singular points in the closed upper half-plane. b) The flow near equilibrium E_1. c) The flow near equilibrium E_4.

To analyze E_2 and E_3 we project the flow on the local chart $U_y^+ = \{(x, y, z) \in \mathbb{S}^2 | y > 0\}$ onto the plane $Y = 1$,

$$\begin{aligned} \dot{x} &= \alpha x^2 + \eta\alpha x - \eta z^3 + (-\eta\alpha + \eta x - \gamma x)z^2 + (\eta\alpha x + x^2 + \eta x)z, \\ \dot{z} &= z(-\gamma z^2 + \alpha x + xz). \end{aligned} \tag{4.11}$$

E_2 and E_3 are in bijective correspondence with points $\tilde{E}_2 = (x, z) = (-\eta, 0)$ and $\tilde{E}_1 = (x, z) = (0, 0)$, respectively, on $Y = 1$ plane. The linearization of (4.11) at $\tilde{E}_2$ has a double negative eigenvalue $\lambda_{1,2} = -\alpha\eta$, therefore $\tilde{E}_2$ is a hyperbolic equilibrium and is an attractor. The linearization of (4.11) at $\tilde{E}_3$ has a zero eigenvalue and an eigenvalue which is equal to $\alpha\eta$ that corresponds to the flow on the equator. In order to determine the nature of this equilibrium, we study the flow restricted to the local center manifold

$$W^{\mathrm{c}}(E_3) = \{(x, z) | x = z^2 + \mathrm{O}(z^3)\}, \tag{4.12}$$

which is given by the following equation

$$\dot{z} = (\alpha - \gamma)z^3 + \mathrm{O}(z^3). \tag{4.13}$$

Since $\alpha < \gamma$ within this region and we are interested in the flow that corresponds to the top of the sphere ($z \geq 0$), we conclude that $\tilde{E}_3$ is a saddle.

To analyze the behavior of the equilibrium E_1 we project the vector field using local chart $U_x^+ = \{(x, y, z) \in \mathbb{S}^2 | x > 0\}$ of the Poincaré sphere onto the plane $X = 1$, thus obtaining

$$\begin{aligned} \dot{y} &= -\alpha y^2(\eta y + 1) + \eta y z^3 - y(-\eta\alpha y - \gamma + \eta)z^2 - y(1 + \eta\alpha y + \eta y)z, \\ \dot{z} &= -\eta z(\alpha y + z)(-z^2 + z + y). \end{aligned} \tag{4.14}$$

On this local chart E_1 is represented by a point $\tilde{E}_1 = (y, z) = (0, 0)$. Note that the linearization of (4.14) about $\tilde{E}_1$ is identically equal to zero, so $\tilde{E}_1$ (and, thus, E_1) is a degenerate equilibrium. To study this degenerate equilibrium of (4.14) at the origin, we perform the quasi-homogeneous blow-up with the coordinate transformation

$$\phi : \mathbb{S}^1 \times \mathbb{R} \to \mathbb{R}^2, \quad ((\bar{z}, \bar{y}), r) \mapsto (z, y), \tag{4.15}$$

where $\bar{z}^2 + \bar{y}^2 = 1$ and

$$z = r\bar{z}, \quad y = r\bar{y}. \tag{4.16}$$

We use charts on $\mathbb{S}^1$ to calculate the flow near E_4 on the top of the sphere ($z \geq 0$) that corresponds to the upper half plane ($y \geq 0$). At first we consider the directional blow-up

$$z = r, \quad y = r\bar{y} \tag{4.17}$$

in the $z > 0$ direction. In blow-up coordinates (4.17), differential equations (4.14) become

$$\begin{aligned} \dot{r} &= r^3\eta(-1 - \bar{y} + r)(1 + \alpha\bar{y}), \\ \dot{\bar{y}} &= -r\bar{y}(-\gamma r + 1 + \alpha\bar{y}). \end{aligned} \tag{4.18}$$

An appropriate rescaling of the independent variable leads to the following system

$$\begin{aligned} \dot{r} &= r^2\eta(-1 - \bar{y} + r)(1 + \alpha\bar{y}), \\ \dot{\bar{y}} &= -\bar{y}(-\gamma r + 1 + \alpha\bar{y}). \end{aligned} \tag{4.19}$$

The system (4.19) has two equilibria: $E_4^1(0, 0)$ with eigenvalues 0 and -1 and $E_4^2(0, -\frac{1}{\alpha})$ with eigenvalues 0 and 1. We will not consider $E_4^2(0, -\frac{1}{\alpha})$ since its nature determines the flow in

the lower half-plane. However, the semi-hyperbolic equilibrium $E_4^1(0,0)$ is of interest to us and it corresponds to the intersection point of the equator and the positive x-axis. On the invariant line $\bar{y}=0$ (4.19) becomes $\dot{r}=-r^2$, which corresponds to the flow on the positive x-axis. When $r=0$, the flow of (4.19) is given by $\dot{\bar{y}}=-\bar{y}(1+\alpha\bar{y})$ which shows that the flow on the blown-up circle within the first quadrant along which $E_4^1(0,0)$ is attracting. Next we use directional blow up coordinates

$$z=r\bar{z}, \quad y=r, \tag{4.20}$$

to blow-up the origin in the $y>0$ direction. With (4.20) differential equations (4.14) become

$$\begin{aligned}\dot{\bar{z}} &= r\bar{z}(-\gamma r\bar{z}^2+\bar{z}+\alpha),\\ \dot{r} &= -r^2(z+\alpha-(-\alpha\eta\bar{z}+\gamma\bar{z}^2-\eta\bar{z}^2-\eta\bar{z}-\alpha\eta)r-\alpha(\eta\alpha\bar{z}^2+\eta\bar{z}^3)r^2).\end{aligned} \tag{4.21}$$

We then desingularize (4.21) by rescaling with respect to the independent variable to obtain

$$\begin{aligned}\dot{\bar{z}} &= \bar{z}(-\gamma r\bar{z}^2+\bar{z}+\alpha),\\ \dot{r} &= -r(z+\alpha-(-\alpha\eta\bar{z}+\gamma\bar{z}^2-\eta\bar{z}^2-\eta\bar{z}-\alpha\eta)r-\alpha(\eta\alpha\bar{z}^2+\eta\bar{z}^3)r^2).\end{aligned} \tag{4.22}$$

The system (4.22) has an equilibrium at $E_4^3(0,0)$ which is a saddle with eigenvalues $\pm\alpha$ and a semi-hyperbolic equilibrium at $E_4^4(-\alpha,0)$ which is not relevant to the flow in the first quadrant of the vector field. Direct examination of (4.22) shows that equilibrium $E_4^3(0,0)$ is attracting along the invariant line $\bar{z}=0$, which corresponds to the flow on the equator, and is repelling along the $r=0$, which is consistent with our analysis above. Combining the information obtained from the analysis of the flow on two charts we conclude that there is a stable parabolic sector at E_4 that belongs to the upper-half plane (see Fig. 4.4, panels c) and a)).

To study E_1, we use another local chart. More precisely, the flow projected from the local chart $U_x^-=\{(x,y,z)\in\mathbb{S}^2|x<0\}$ of the Poincaré sphere onto the plane $X=-1$ is given by

$$\begin{aligned}\dot{y} &= -\eta yz^3+(-\alpha\eta y^2-\eta y+\gamma y)z^2+(-\alpha\eta y^2-\eta y^2+y)z-\alpha\eta y^3+\alpha y^2,\\ \dot{z} &= -\alpha\eta zy^2+(-\alpha\eta z^3-\alpha\eta z^2-\eta z^2)y-\eta z^4-\eta z^3.\end{aligned} \tag{4.23}$$

Note that E_1, which is the antipodal to E_4, as it is expected, is a degenerate equilibrium with zero linear part. To analyze the flow near E_1 on the upper half-plane, we perform the quasi-homogeneous blow-up with the coordinate transformation (4.16). We consider the directional blow-up (4.20) in the $y>0$ direction. The differential equations (4.23) in these coordinates become

$$\begin{aligned}\dot{r} &= -r^2(\alpha\eta r^2\bar{z}^2+\eta r^2\bar{z}^3+\alpha\eta r\bar{z}+\eta r\bar{z}^2-\gamma r\bar{z}^2+\alpha\eta r+\eta r\bar{z}-\alpha-\bar{z}),\\ \dot{\bar{z}} &= -r\bar{z}(\gamma r\bar{z}^2+\alpha+\bar{z}).\end{aligned} \tag{4.24}$$

We rescale the independent variable in (4.24) by r and obtain

$$\begin{aligned} \dot{r} &= -r(\alpha\eta r^2\bar{z}^2 + \eta r^2\bar{z}^3 + \alpha\eta r\bar{z} + \eta r\bar{z}^2 - \gamma r\bar{z}^2 + \alpha\eta r + \eta r\bar{z} - \alpha - \bar{z}), \\ \dot{\bar{z}} &= -\bar{z}(\gamma r\bar{z}^2 + \alpha + \bar{z}). \end{aligned} \tag{4.25}$$

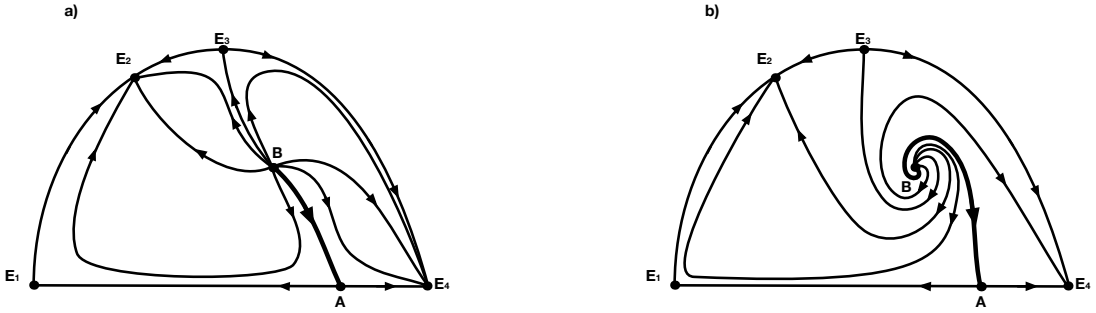

FIGURE 4.5. The flow on the upper-half of the Poincaré disk; a) Region 4A, b) Region 4B.

The system (4.25) has a saddle equilibrium $E_1^1 = (0, 0)$ with eigenvalues $\pm\alpha$ and $E_1^2 = (0, -\alpha)$ with eigenvalues 0 and 1 that correspond to the equilibria on the blown-up circle. Equilibrium $E_4^1(0, 0)$ is attracting along the line $\bar{z} = 0$. The flow of (4.25) restricted to the invariant line $r = 0$ is given by $\dot{\bar{z}} = -\bar{z}(\alpha + \bar{z})$, therefore E_1^1 is attracting along this line. This information extends to the flow on the sector of the blown-up circle that belongs to the first quadrant. Equilibrium E_1^1 is repelling along the line $\bar{z} = 0$ due to the reduced flow $\dot{r} = \alpha r$ that implies the behavior of the flow on the equator of the Poincaré sphere.
Next we use directional blow up coordinates (4.17) to blow-up the origin in the $z > 0$ direction. With (4.17) differential equations (4.23) become

$$\begin{aligned} \dot{\bar{y}} &= r\bar{y}(\alpha\bar{y} + \gamma r + 1), \\ \dot{r} &= -r^3\eta(\alpha r\bar{y} + \alpha\bar{y}^2 + \alpha\bar{y} + r + \bar{y} + 1). \end{aligned} \tag{4.26}$$

We desingularize (4.26) by rescaling with respect to the independent variable and obtain

$$\begin{aligned} \dot{\bar{y}} &= \bar{y}(\alpha\bar{y} + \gamma r + 1), \\ \dot{r} &= -r^2\eta(\alpha r\bar{y} + \alpha\bar{y}^2 + \alpha\bar{y} + r + \bar{y} + 1). \end{aligned} \tag{4.27}$$

We consider only the equilibrium $E_1^3 = (0, 0)$ of this system, which is semi-hyperbolic with eigenvalues 1, 0. The flow of (4.27) on the invariant line $\bar{y} = 0$, which corresponds to the x-axis, is given by $\dot{r} = -\eta r^2(1 + r)$, therefore E_1^3 is attracting along this line. The flow on the invariant line $r = 0$ corresponds to the flow on the segment of the blown-up circle that

connects E_1^3 to E_1^1 and is given by $\dot{\bar{y}} = \bar{y}(1 + \alpha\bar{y})$ which is consistent with our analysis of the flow of (4.25) above. Combining our analyses of the flow on two charts $y > 0$ and $z > 0$ given by (4.25) and (4.27) (those cover the segment of the blown-up circle that belongs to the first quadrant) we conclude that there is a hyperbolic sector at E_1 that belongs to the upper half-plane (see Fig. 4.4, panels b) and a)).

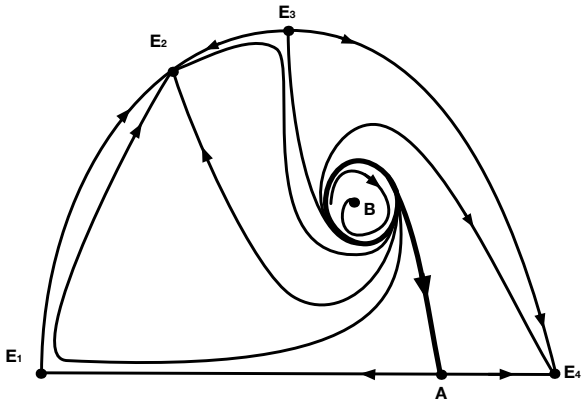

FIGURE 4.6. Illustration for Theorem 4C.

The information gathered from compactification and the information about the heteroclinic orbit obtained through the Singular Perturbation Theory combined with Poincaré - Bendixon Theorem identify the flow on the upper half-plane of the phase plane in each parameter regime described in Theorems 4.2, 4.3, and 4.4 as one that corresponds to panels a), b) in Fig. 4.5, and Fig. 4.6, respectively. The heteroclinic orbit that connects the unstable node at B with a saddle at A persists as a heteroclinic orbit (see panel a) in Fig. 4.5) as η changes from Region 4A to Region 4B as the equilibrium B changes from unstable node to an unstable spiral (see panel b) in Fig. 4.5). Upon crossing of η to Region 4C, the equilibrium at B undergoes a subcritical Hopf bifurcation (Fig. 4.6), thus creating an heteroclinic orbit that asymptotically connects the saddle at A to the unstable periodic orbit around B. In addition, within Region 4C, a manifold of orbits exists that connect the unstable periodic orbit to the stable equilibrium at B (a sink). The proof of the Theorems 4.2, 4.3, and 4.4 is completed.

Acknowledgements. This work was partially supported by the NSF grant DMS-1311313 (to Ghazaryan) and a grant from the Simons Foundation (#246535 to Manukian).

References

[1] A. A. Andronov, E. A. Leontovich, I. I. Gordon, A. A. Maier, *Theory of Bifurcations of Dynamical Systems on a plane*, Israel Program for Scientific Translations, Jerusalem, 1971.

[2] C. Chicano, *Ordinary differential equations with applications*, Springer Texts in Applied Mathematics, 34, 2006.

[3] C. Chicone, J. Sotomayor, *On a Class of Complete Polynomial Vector Fields in the Plane.* J. Dif. Equations **61** (1986), 398-418.

[4] E. J. Doedel, R. C. Paffenroth, A. Champneys, T. F. Fairgrieve, Y. A. Kuznetsov, B. E. Oldman, B. Sandstede, and X. Wang 2001 AUTO 2000: continuation and bifurcation software for ordinary differential equations (with Hom- Cont). Technical report, Concordia University (http://indy.cs.concordia.ca/auto/).

[5] G. F. D. Duff, *Limit-cycles and rotated vector fields*, Analysis of Mathematics, **57** (1953), 15-31.

[6] F. Dumortier, J. Llibre, J. C. Artés, *Qualitative Theory of Planar Differential Systems*, Springer, Berlin, 2006.

[7] N. Fenichel, *Geometric singular perturbation theory for ordinary differential equations*, J. Differential Eqs. **31** (1979), 53-98.

[8] C. K. R. T. Jones, *Geometric singular perturbation theory*, in Dynamical Systems (Montecatini Terme, 1994), Lecture Notes in Math. **1609**, Springer, Berlin, 1995, 44-118.

[9] Q. X. Liu, A. Doelman, V. Rottschäfer, M. de Jager, P. M. Herman, M. Rietkerk, J. van de Koppel, *Phase separation explains a new class of self-organized spatial patterns in ecological systems,* Proc Natl. Acad. Sci USA. **110** (2013), 11905-11910.

[10] Q. X. Liu, E. J. Weerman, P. M. Herman, H. Olff, J. van de Koppel, *Alternative mechanisms alter the emergent properties of self-organization in mussel beds,* Proc. Biol. Sci. **279** (2012), 2744-2753.

[11] L. M. Perko, *Rotated vector fields*, J. Diff. Eqns, **103** (1993), 127-145.

[12] L. M. Perko, *Differential Equations and Dynamical Systems*, second edition, Springer Texts in Applied Mathematics, 1998.

[13] J. van de Koppel, M. Rietkerk, N. Dankers, and P. M. J. Herman, *Scale-dependent feedback and regular spatial patterns in young mussel beds.* Am. Nat. **165** (2005), E66-E77.

[14] R. -H. Wang, Q. -X. Liu, G. -Q. Sun, Z. Jin, and J. van de Koppel. Nonlinear dynamic and pattern bifurcations in a model for spatial patterns in young mussel beds. J. R. Soc. Interface **6** (2009), 705-718.

Department of Mathematics, Miami University
E-mail address: ghazarar@muohio.edu

Department of Mathematics, Miami University
E-mail address: manukive@muohio.edu